









Experimental Evaluation of 1 kW-class Prototype REBCO Fully Superconducting Synchronous Motor Cooled by Subcooled Liquid Nitrogen for E-Aircraft

Hiromasa Sasa , Masataka Iwakuma , Koichi Yoshida, Seiki Sato, Teruyoshi Sasayama , Takashi Yoshida , Kaoru Yamamoto , Shun Miura , Akifumi Kawagoe , Teruo Izumi , Akira Tomioka, Masayuki Konno, Yuichiro Sasamori, Hirokazu Honda, Yoshiji Hase, Masao Syutoh, Sergey Lee, Shinya Hasuo, Miyuki Nakamura, Takayo Hasegawa, Yuhji Aoki, and Takahiro Umeno

Abstract—For the development of electric propulsion aircrafts with light weight, low emission and high efficiency, MW-class fully superconducting synchronous machines operating at liquid nitrogen temperature were conceptually designed with REBa₂Cu₃O_{7-δ} (REBCO) superconducting tapes in our previous studies. To verify the actualization of the structure and cooling method, a 1 kW-class prototype fully superconducting synchronous motor was designed and constructed in this study. The fixed armature was cooled with subcooled liquid nitrogen at 65 K. The rotor was cooled with helium gas. The pole number was two for the future high speed operation. The applicability of the complicated casing structure with three chambers into fully superconducting motor was also investigated from the viewpoint of thermal insulation. The operations as a motor up to 500 rpm and a generator demonstrated that the designed structure and cooling method were reasonable and effective for cooling the fixed armature and rotating field windings.

Index Terms—Fully-superconducting motor, electric aircraft, REBCO, subcooled liquid nitrogen.

Manuscript received November 25, 2020; revised January 7, 2021, January 15, 2021, and January 17, 2021; accepted January 25, 2021. Date of publication January 29, 2021; date of current version March 16, 2021. This work was supported in part by based on results obtained from a Project Commissioned by the New Energy and Industrial Technology Development Organization (NEDO), in part by the Japan Science and Technology Agency (JST): Advanced Low Carbon Technology Research and Development Program (JPMJAL1405), and in part by the Japan Society for the Promotion of Science (JSPS): Grant-in-Aid-for Scientific Research (JP18H03783 and JP19K14964). (*Corresponding author: Hiromasa Sasa.*)

Hiromasa Sasa, Masataka Iwakuma, Koichi Yoshida, Seiki Sato, Teruyoshi Sasayama, Takashi Yoshida, Kaoru Yamamoto, and Shun Miura are with the Institute of Superconductors Science and Systems, Kyushu University, Fukuoka 819-0395, Japan (e-mail: sasa.hiromasa.379@s.kyushu-u.ac.jp).

Akifumi Kawagoe is with the Kagoshima University, Kagoshima 890-0065, Japan.

Teruo Izumi is with the National Institute of Advanced Industrial Science and Technology, Tsukuba 305-8560, Japan.

Akira Tomioka, Masayuki Konno, Yuichiro Sasamori, Hirokazu Honda, Yoshiji Hase, and Masao Syutoh are with Fuji Electric Company Ltd., Ichihara 290-8511, Japan.

Sergey Lee, Shinya Hasuo, and Miyuki Nakamura are with SuperOx Japan, LLC, Sagami-hara 252-0243, Japan.

Takayo Hasegawa and Yuhji Aoki are with SWCC Showa Cable System Company LTD., Sagami-hara 229-1133, Japan.

Takahiro Umeno is with Taiyo Nippon Sanso Corporation, Tsukuba 305-2611, Japan.

Color versions of one or more figures in this article are available at <https://doi.org/10.1109/TASC.2021.3055452>.

Digital Object Identifier 10.1109/TASC.2021.3055452

I. INTRODUCTION

IT IS predicted that the air traffic demand for all of the world in 2039 will grow up to 2.2 times larger than in 2019 [1]. The aviation emission is one of the serious problems which enhance the global warming. The international civil aviation organization set a goal of improvement of the global annual average fuel efficiency in a rate of 2% per year [2]. Moreover, the international air transport association aims to improve aviation fuel efficiency to reduce carbon emissions in 2050 to half of that in 2005 [3]. To achieve these purposes, replacing the existing propulsion system containing jet engines by the electric propulsion system is one of the promising solutions [4], [5] and many research groups are investigating the electric aircraft with superconducting rotating machines [6]–[10]. However, the conventional rotating machines composed of iron cores and copper windings are too heavy to satisfy the stringent weight requirement of aircraft applications. Therefore, it is required that development of the superconducting rotating machine which has advantage of light weight, low emission, low noise, high efficiency and so on. Introducing the superconducting machines such as motors, generators, transformers, and so on is the most effective approach to realize e-aircraft, which is the future aircraft with electric propulsion system. Our research group has designed and constructed a 1 kW-class fully superconducting synchronous motor for the 1st step of the national project, “Development of innovative electric propulsion systems for aircrafts”, funded by NEDO. Fig. 1 shows the photograph of the motor. Both of field and armature windings are wound by REBa₂Cu₃O_{7-δ} (REBCO, RE = Rare Earth, such as Y, Eu, Gd, etc.) superconducting wires. The REBCO tape has the advantage of high critical current density property in magnetic field. The armature windings and the field windings were cooled by the subcooled liquid nitrogen and the cool gas helium, respectively. This paper reports the results of evaluation tests. The temperature variations of the coils were observed through the cooling process. After cooling, the *I-V* characteristics of the respective windings were measured. Furthermore, the motor was operated up to 500 rpm successfully.

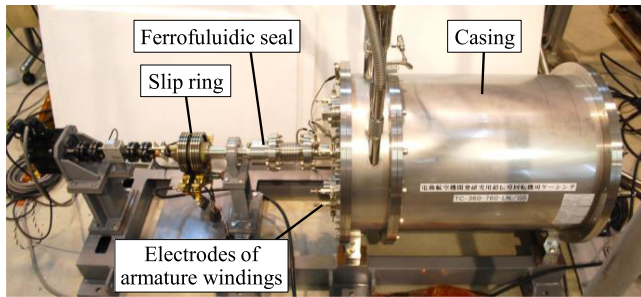


Fig. 1. Photograph of 1 kW-class fully superconducting synchronous motor.

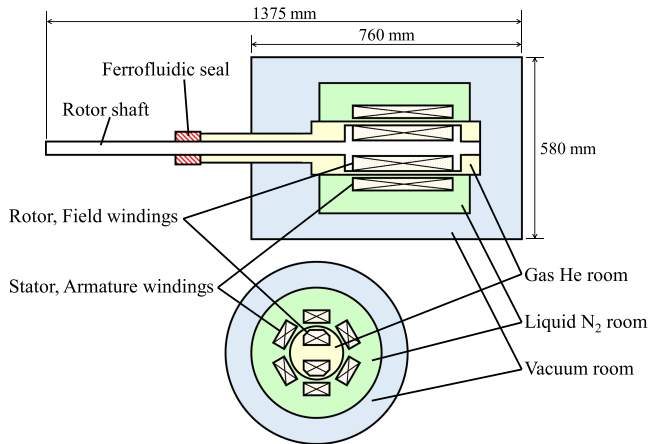


Fig. 2. Schematic illustrations of casing structure of 1 kW-class fully superconducting synchronous motor.

II. DESIGN AND CONSTRUCTION OF MOTOR

A. Casing Structure

Most parts of the motor casing were made of nonmagnetic stainless steel, SUS304. The total weight of the casing was approximately 300 kg. The reduction of the weight is the future task. The casing is separated into three rooms as illustrated in Fig. 2. In Fig. 2, the pipelines to inject and withdraw coolant are omitted. Each coolant room in the motor has two pipelines. Two kinds of cooling methods were adopted for the superconducting windings. The outermost room was vacuum for thermal insulation between outer atmosphere and inner coolant.

The armature winding was installed into the middle room. It was cooled by subcooled liquid nitrogen which was circulated by the cooling system shown in the next subsection. There are two reasons for adoption of that as coolant. One of the reasons of the adoption of subcooled liquid nitrogen is that a huge AC loss is induced in the superconducting armature winding. The armature winding is subject to the rotating magnetic fields which are generated by itself and the rotating field winding. It can cause serious problems such as quench due to a temperature rise. A high capacity of cooling is required for the stable armature operation. The second reason is the enhancement of the critical current, I_C , property of the REBCO windings. Operating the armature windings at lower temperature, larger

current is allowed, and then the larger output power of motor is expected. In case of our motor, 65 K of nitrogen whose temperature is enough higher than the freezing point (~ 63 K) was used from the viewpoint of light weight and also safety due to good cooling. To utilize higher current capacity of REBCO windings in magnetic field, especially for future bigger motor with high output power such as MW-class, lower operating temperature is recommended. For superconducting machines at low temperature, liquid neon, liquid hydrogen, and the others are the options of coolant. However, these coolants are not suitable for aircraft applications because of following reasons. The superconducting machines in electric propulsion systems for aircraft needs to take the lightning accidents into account. When quench by such accident occurred in superconducting winding immersed in liquid coolant, that liquid boils and then the coolant consists of mixture of liquid state and gas state. According to the data [11], the breakdown voltage of gas neon is 1/60 of that of gas nitrogen. Neon with such dielectric strength property is not suitable for e-aircraft. Liquid hydrogen is not cleared whether it can maintain the superconducting state of the windings in case of lightning surge even by its low specific heat capacity at low temperature. Therefore, our project chose liquid nitrogen as the best coolant for aircraft application.

The field winding was installed into the innermost room and are cooled by helium gas. During operation, the helium gas is kept at low temperature by heat exchange with the liquid nitrogen in the middle room through the wall which separates the rooms. In the field winding, little AC loss is induced since the applied magnetic field is mainly DC. AC magnetic field due to the armature winding is much smaller than the self DC field. In addition, the coolant for the field windings, i.e., the rotor, should have low windage loss, because it rotates in high speed during operation. The helium gas was injected into the motor at the cooling step, and then it has been kept sealed during experiments. The pressure of the helium gas was not controlled, so that it was almost atmospheric pressure. The rotor shaft is supported by two ball bearings. One of them is at the far side of the ferrofluidic seal. Another one is at edge of the shaft at inside of the motor casing. That bearing uses no oil because it has to be normal even at low temperature.

The rotor shaft is required good thermal insulation capacity to mitigate the heat flow into the motor casing, and it is one of the key technologies of designing and manufacturing superconducting motor. In this paper, the thermal insulation structure of rotor shaft of our motor is not explained in detail because it involves the subject matter of patent.

B. Subcooling and Circulating System for Liquid Nitrogen

Fig. 3 shows the schematic illustration of the system used for liquid nitrogen to be subcooled and circulated. This system can be regarded as consisting of two parts which are the subcooler bath and the circulation loop. The heat exchanger as a part of circulation loop was soaked in liquid nitrogen in the subcooler bath during experiment. The inner pressure of subcooler bath was controlled by external decompression pump to keep the

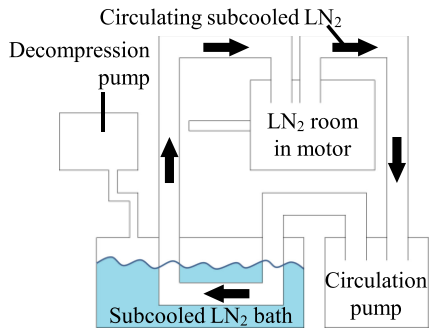


Fig. 3. Schematic illustrations of cooling and circulating system for liquid nitrogen.

TABLE I
SPECIFICATIONS OF REBCO SUPERCONDUCTING TAPES

Winding	Armature	Field
Provider	AIST	SuperOx Japan
Width	5 mm	4 mm
Thickness	113 μm	89 μm
Superconducting layer	EuBCO + BHO (3.5 mol%)	EuBCO
I_c at 77 K, self-field	> 300 A	> 100 A

liquid nitrogen subcooled state. In case of 65 K of the liquid nitrogen, the inner pressure of the bath was approximately 4×10^4 Pa. The liquid nitrogen was circulated in the loop and cooled the superconducting windings in the motor in following procedure.

- 1) The circulation pump forces the liquid nitrogen to keep flowing around in the loop.
- 2) The liquid nitrogen passes through the heat exchanger in the subcooler bath and it is cooled.
- 3) The liquid nitrogen goes into the motor casing. Then it cools the armature windings.
- 4) The liquid nitrogen goes back to the circulation pump.
- 5) Back to 1.

The flow rate of the circulation pump was 18 liter per minute. The cooling capacity of this system is 2 kW.

C. Ferrofluidic Seal on Rotating Shaft

The ferrofluidic seal was adopted for sealing between the helium gas room and outer atmosphere, and it is on the shaft as shown in Fig. 2. For the purpose of maintaining its sealing capacity, the ferrofluidic seal needs to be kept room temperature not to be frozen. Therefore, the heat insulation property of the rotating shaft is important.

D. Electrical Specifications

The specifications of the adopted REBCO superconducting tapes are listed in Table I, and the designed specifications of the motor are listed in Table II. Please note that the parameters written in Table II don't indicate the experimental conditions. For example, though the designed rated rotation speed is 625 rpm, the experiments in this study was conducted with 500 rpm

TABLE II
DESIGNED SPECIFICATIONS OF MOTOR

	1 kW-class
Output power	1 kW-class
Rated rotation speed	625 rpm (10.4 Hz)
Number of poles	2
Rated line voltage	25 V_{rms}
Rated current	100 A_{rms}
Field current	100 A
Operation temperature	65 K
Electrical gap	29.9 mm
Number of coils: Armature	6
Field	2
Winding number: Armature	80 turn / coil
Field	358 turn / coil
Effective length	220 mm
Inner diameter of stator	172 mm

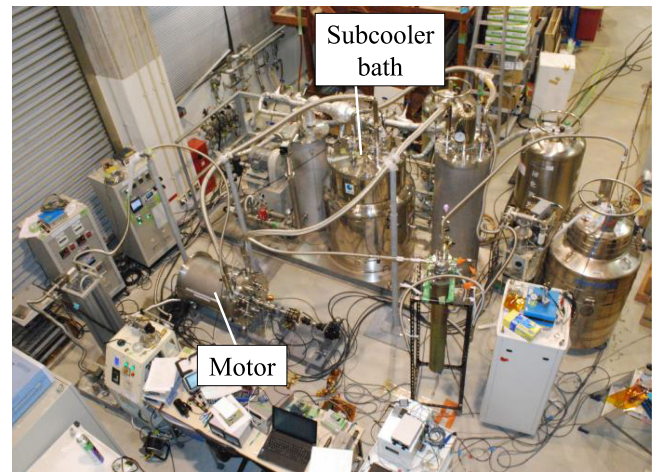


Fig. 4. Photograph of experimental system for 1 kW-class fully superconducting synchronous motor.

rotation by reason of safety of laboratory equipment. To estimate the AC loss in the superconducting windings, the magnetic field applied to them during rated operation was calculated by using JMAG, a software for electromagnetic analysis by finite element method. The maximum value of the amplitude of the magnetic field applied to the windings is 0.3 T. Using an estimation method [12], the AC loss is estimated as 38 W. In addition, the eddy current loss in the wall of SUS304 which surrounds the liquid nitrogen room was calculated by JMAG as 607 W. Therefore, the cooling system explained above has sufficient cooling capacity. In future motor, larger magnetic field is applied to the casing and larger eddy current loss might be induced especially in the wall between armature and field windings. Therefore, in the future work, the suitable material for the casing structure should be discussed for not only light weight design but also reduction of loss.

III. EXPERIMENTAL SETUP

Fig. 4 shows the photograph of the entire experimental system. Three types of experiments as below were conducted.

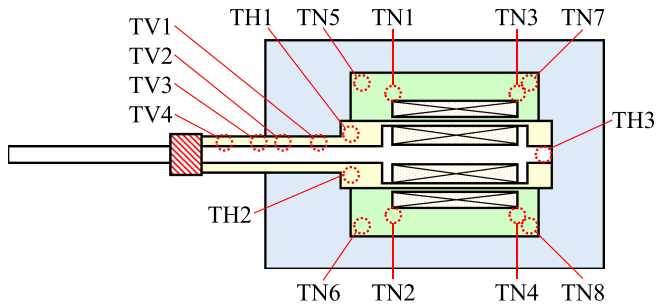


Fig. 5. Schematic illustration of the motor cross section in which the positions of the temperature sensors are indicated.

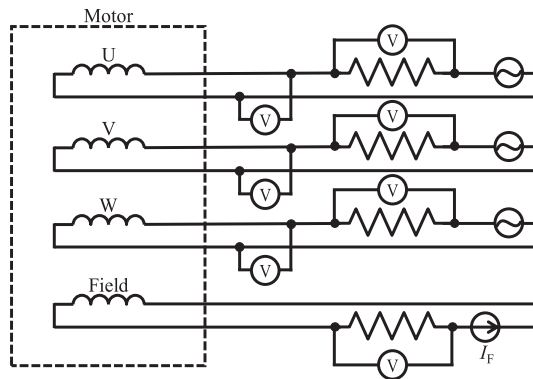


Fig. 6. Circuit diagram for motor operation test.

A. Cooling Property

To verify the applicability of the casing structure explained above for superconducting synchronous motor, fourteen temperature sensors were attached as shown in Fig. 5 and the temperature in the casing was observed during cooling process. The rotor was not rotated during cooling process.

B. I-V Characteristics of Superconducting Windings

After cooling, I-V characteristics of six armature coils and two field coils were observed in advance of motor operation.

C. Motor Operation Test

Each armature winding was connected to the individual bipolar power supplies so that three-phase AC power was provided. Fig. 6 shows the circuit diagram for motor operation.

IV. EXPERIMENTAL RESULTS

A. Cooling Property

The observed temperature variations at the respective positions shown in Fig. 5 during cooling process are shown in Fig. 7.

The temperature of the circulated liquid nitrogen was set to 65 K. The motor was cooled from room temperature to LN2 temperature in 30 hours. Fig. 8 shows the temperature distribution in the motor in a steady state, which is indicated

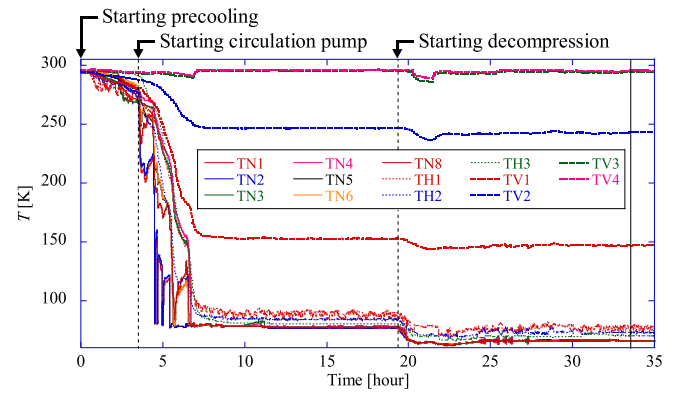


Fig. 7. Temperature variations in the motor during cooling process. The temperatures at the time presented by vertical solid line is shown in Fig. 8.

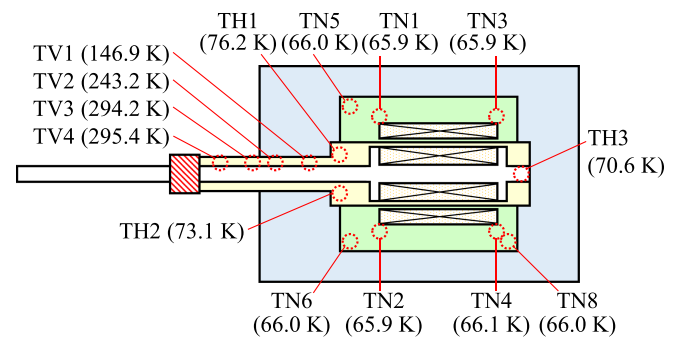


Fig. 8. Temperature distribution in the motor in a steady state after cooling.

by the vertical line in Fig. 7. The temperatures in the liquid nitrogen room were almost uniform as ranged from 65.9 K to 66.1 K. On the other hand, the temperatures in the gas helium room were ranged from 70.6 K to 76.2 K. After observing such nonuniform temperature distribution in the gas helium room, a servo motor was attached to the end of the shaft, and stirring of the rotor was started in 100 rpm with an anticipation of more uniform distribution. Then the temperatures at TH1, TH2 and TH3 varied to 69.4 K, 70.8 K and 67.1 K, respectively. The temperature moved lower, and the variation range decreased from 5.6 K to 3.7 K. In both cases before and after stirring, the temperatures at TH1 and TH2 which are near the shaft were higher than at TH3. It is predicted that the heat conduction from the room temperature through the shaft caused such temperature distribution. The temperature in the gas helium room is slightly higher than in the liquid nitrogen room, but it cannot be a serious problem because it was much lower than the critical temperature of the REBCO tapes (>90 K). However, the degradation of I_C is caused by temperature rise. This should be improved.

Furthermore, we focused on the temperature distribution on the rotor shaft. The observed temperature distribution on the shaft is plotted in Fig. 9. We can see that the temperature varies from room temperature to LN2 temperature linearly. It shows that the design of the thermal insulation including the shaft is optimized in moderation. The ferrofluidic seal was kept room temperature successfully.

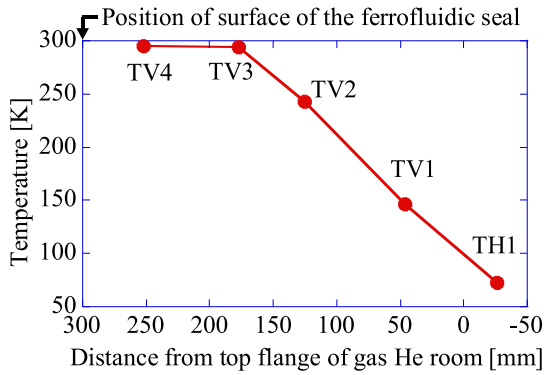


Fig. 9. Temperature distribution of the vicinity of the rotor shaft.

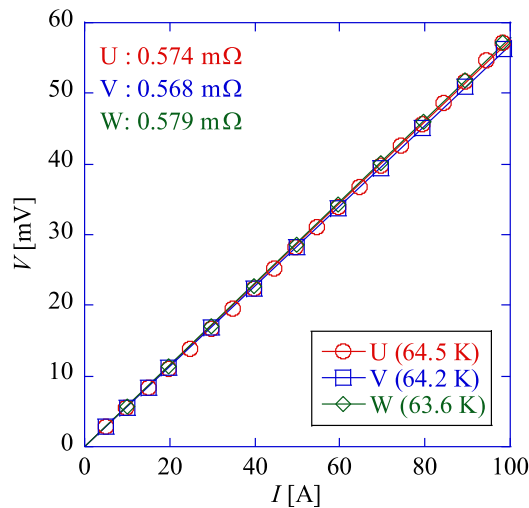


Fig. 10. Observed I - V characteristics of the armature windings. The temperatures in the parentheses in the legend indicate the temperatures in liquid nitrogen room at the time when the measurements were conducted.

B. I - V Test of Superconducting Windings

The measurements of I - V characteristics of the armature windings were conducted individually for each phase windings. The obtained I - V characteristics are shown in Fig. 10. It was confirmed that any armature winding had no voltage rise at least at 100 A operation. The linear voltages were generated at the electrodes and the connections between the electrodes and the superconducting tapes. The windings were already equipped in the motor at that moment and it was difficult to take the complicated casing structure apart to repair or replace them. Considering the risk of accident such as quench, the I_C measurement of the REBCO windings was not conducted.

C. Motor Operation Test

The motor was operated with no load. The smooth rotation up to 500 rpm was confirmed. Considering the safety of the operation and further successive tests, the transport currents were restricted within the rated value. Fig. 11 shows the temperature variation during motor operation test. There were no temperature rises owing to current in the windings and the rotation of

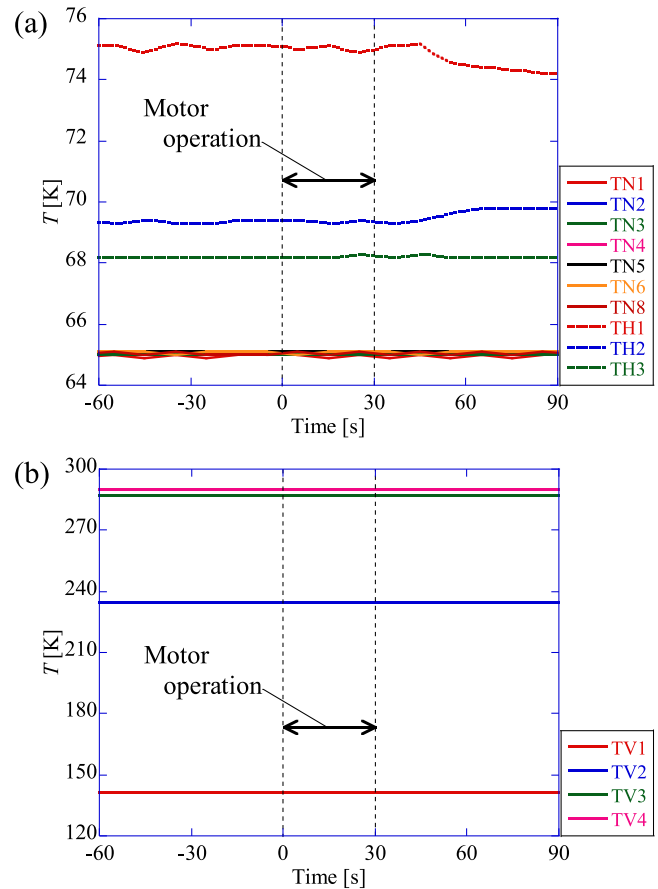


Fig. 11. Temperature variations in the motor during motor operation test.

the rotor. This result shows that the cooling structure of this motor was optimized for motor operation.

V. CONCLUSION

A 1 kW-class fully REBCO superconducting synchronous motor was designed and constructed for the purpose of the confirmation of the validity of the designed motor structure and cooling method for fully superconducting rotating machines for e-aircrafts. The obtained results demonstrate the follows. The fully superconducting synchronous motor was successfully operated up to 500 rpm. The cooling system using the subcooled liquid nitrogen showed good performance for cooling the armature winding with a high density of AC loss. On the other hand, nonuniform temperature distribution in the rotor room was also observed. In future work, the temperature distribution should be investigated in detail, and the solutions for improvement will be proposed. One of the options of them is installing a fan in that room to make wind flow and to cool the windings positively. Moreover, we are considering modification of the current lead for the field windings, because there are larger loss generates in case of future bigger motor. The outcome is a great achievement for the development of superconducting propulsion systems for e-aircraft.

We are now designing a REBCO fully superconducting motor with 500 kW output power as a next stage.

REFERENCES

- [1] Japan Aircraft Development Corporation, "Worldwide market forecast 2020-2039 (Provisional release)," 2020, Accessed on: Oct. 5, 2020. [Online]. Available: http://www.jadc.jp/files/topics/157_ext_01_en_0.pdf
- [2] G. G. Fleming and U. Ziegler, "Environmental trends in aviation to 2050," in *Proc. ICAO Environ. Rep.: Aviation Climate Change*, 2013, pp. 22–27.
- [3] International Air Transport Association, "Halving emissions by 2050 - aviation brings its targets to copenhagen," 2009, Accessed on: Oct. 5, 2020. [Online]. Available: <https://www.iata.org/en/pressroom/pr/2009-12-08-01/>
- [4] C. A. Luongo *et al.*, "Next generation more-electric aircraft: A potential application for HTS superconductors," *IEEE Trans. Appl. Supercond.*, vol. 19, no. 3, pp. 1055–1068, Jun. 2009.
- [5] F. Berg, J. Palmer, P. Miller, M. Husband, and G. Dodds, "HTS electrical system for a distributed propulsion aircraft," *IEEE Trans. Appl. Supercond.*, vol. 25, no. 3, Jun. 2015, Art. no. 5202705.
- [6] T. Balachandran, D. Lee, N. Salk, and K. S. Haran, "A fully superconducting air-core machine for aircraft propulsion," *IOP Conf. Ser.: Mater. Sci. Eng.*, vol. 756, 2020, Art. no. 012030.
- [7] D. Dezhin, I. Dezhina, and R. Ilyasov, "Superconducting propulsion system with LH2 cooling for all-electric aircraft," *J. Phys.: Conf. Series*, vol. 1559, 2020, Art. no. 012143.
- [8] F. Grilli *et al.*, "Superconducting motors for aircraft propulsion: The advanced superconducting motor experimental demonstrator project," *J. Phys.: Conf. Ser.*, vol. 1590, 2020, Art. no. 012051.
- [9] M. Komiya *et al.*, "Design study of 10 MW REBCO fully superconducting synchronous generator for electric aircraft," *IEEE Trans. Appl. Supercond.*, vol. 29, no. 5, Aug. 2019, Art. no. 5204306.
- [10] Y. Terao, A. Seta, H. Ohsaki, H. Oyori, and N. Morioka, "Lightweight design of fully superconducting motors for electrical aircraft propulsion systems," *IEEE Trans. Appl. Supercond.*, vol. 29, no. 5, Aug. 2019, Art. no. 5202305.
- [11] L. G. Christophorou, "Insulating gases," *Nucl. Instruments Methods Phys. Res. Sect. A*, vol. 268, no. 2/3, 1988, pp. 424–433.
- [12] H. Sasa, S. Miura, M. Iwakuma, T. Izumi, T. Machi, and A. Ibi, "Estimation method for AC loss of perpendicularly stacked REBa₂Cu₃O_y superconducting tapes under magnetic field," *Physica C*, vol. 580, 2021, pp. 1353801.